Dynamic Simulation of Electromagnetic Actuators Based on the Co-Energy Map

A. Espírito Santo, M. R A. Calado, and C. M. P. Cabrita

Department of Electromechanical Engineering
University of Beira Interior, Covilhã, 6201-001, Portugal
aes@ubi.pt, rc@ubi.pt, cabrita@ubi.pt

Abstract ─ The development of new and efficient control methodologies demands the availability of mathematical models for the electromagnetic device under control. These models must be solved with great accuracy and speed. The finite element method (FEM) gives truthful results but computational demanding increases with device geometrical complexity. This paper proposes a new method for dynamic behavior simulation that uses FEM software at its early stage, to obtain the co-energy map for devices concerning static positions for different excitation currents. Inductance and force maps are derived from the co-energy map. A numerical model of a case study is built with Matlab© to obtain device dynamic response. The software implementation procedure is described in detail. The achieved results are compared with the ones obtained from the FEM tool analysis. The small computation effort required by the proposed analysis method makes possible that complex control methodologies can be developed and tested based on the proposed model.

Index Terms ─ Co-energy maps, dynamic behavior, electromagnetic actuator, numerical method.

I. INTRODUCTION

The electromagnetic actuators behavior analysis is nowadays, as in the past [1], a concerning subject for control in engineering areas as robotics or precision actuation. With the introduction of some simplifications, as ignoring material magnetic non-linearity, the analytical analysis of electromagnetic devices is possible only for the simplest geometries. The analysis tasks of actuators with higher structural complexity, with multi-excitation, or intricate geometry is very complex, and it is difficult to obtain an analytical solution. For these situations, the option is always to find the solution through the application of methodologies based on numerical analysis [2-10]. The dynamic behavior of an actuator can also be obtained through the experimental knowledge of the magnetic characteristics, as proposed in [11, 12].

The design of electromechanical devices requires the prediction of the developed force. This knowledge is often derived from field solutions obtained through numerical analysis, based upon different approaches, such as in [13-16]: (1) classical virtual work; (2) Maxwell stress tensor; (3) Coulomb's virtual work. These methods are currently used within the application of finite element analysis [17], but some care must be observed in their application. The mentioned methods can be classified depending on the number of required solutions. The classic method of virtual work requires two or more solutions, turning it computationally demanding. The Maxwell stress tensor and the Coulomb virtual work methods both require only one solution of the problem, making them more computationally efficient.

An issue with the application of the classic virtual work method is that if the moving part of the device performs a small displacement, the variation observed in the co-energy of the system is also small; as a result, a round-off error is introduced. On the other hand, if the displacement is large, a substantial error in the differentiation process is also introduced. These two problems cannot be simultaneously minimized, because one of them cannot be minimized without penalizing the other.

The choice of the method to be used is conditioned by factors such as the computational cost, data consistency, and precision requirements for the results.

The finite element analysis is a widely used numerical method to study electromagnetic problems with irregular and not homogeneous geometries. Finite element algorithms implementations are extremely efficient and commercially available. Nevertheless, these software tools are very expensive and require a large computation time. As a result, these characteristics make the execution of a high number of simulations difficult, with the aim of developing an optimal control strategy.

The aim of the presented work is the development of a new methodology that, applied to an electromechanical device, allows its electrodynamics study. Applying the method proposed here, it is possible to obtain a device dynamical model, based on the co-energy map [18-19]. The method is called dynamic modeling co-energy map (DMC).

This paper is structured as follows: in Section II, a theoretical analysis, based on device electromechanical energy conversion, is presented. The theoretical model possesses two components that describe the energy conversion process. The first one characterizes the electromagnetic process, taking into account the variation in magnetic induction depending on both mechanical displacement and current value. The second one describes the mechanical system. Section III presents a numerical analysis of the electromagnetic actuator, based on a 2D FEM, for the specific knowledge of the device. Several static simulations, for each device's relative position and for different current levels are performed, allowing the construction of a three-dimensional co-energy map. This map is the basis for the knowledge of the attraction force, magnetic flux, and inductance, which define the device numerical model, required for the development of the DMC method. Section IV presents the development details in Matlab© of the proposed method used to observe device dynamical response, in which computation demands are completely independent of the model geometry complexity. In Section V, the results obtained with the application of the proposed methodology, to a chosen case study, are presented. That analysis allows the comparison of the obtained results with the ones obtained with the application of the finite elements tool, when the iron losses are ignored. This allows the validation of the proposed method. Section VI outlines the conclusions.

II. ELECTROMECHANICAL ENERGY CONVERSION

An electromechanical device can convert electrical energy into mechanical energy, or vice--versa. This process is made through the device magnetic field. Different kinds of devices appeal to this principle, and operate according to similar physical processes, for example: transducers used in instrumentation, as the linear variable differential transformer, or actuators used in the electromechanical drives, generally called motors, if they produce force or torque, or generators, in case of producing electrical energy.

Some of the methods to produce force through the use of the electric energy are the following ones: interaction of two magnetic fields, such as a conductor carrying current in a magnetic field; ferromagnetic materials that moves to reduce the reluctance of the magnetic circuit; magnetostriction or deformation of a ferromagnetic material in a magnetic field; piezoelectric effect in the application of an electric potential to a piezoelectric crystal.

The magnetic actuator can be considered as a complete system composed by three sub-systems: (1) the electrical system; (2) the mechanical system; and (3) the coupling field. Note that in spite of the here adopted case study (electrovalve) only allowing longitudinal motion, the device possesses the three previously mentioned sub--systems, and its analysis can provide valuable information about the operation of more complex electro-magneto-mechanical devices.

Looking to the operation principles of an electromechanical device, and the respective process of energy conversion, it can be assumed that, from the energy point of view, three main advantages are presented [20]: (1) the problem formulation is simplified; (2) the analysis methodologies can easily be deduced; and (3) the experimental analysis can be made in order to confirm adopted analysis. For beyond the previous advantages, the application of the classic method of virtual work makes the problem formulation independent from the geometric complexity of the actuator, which can be considerable in some devices.

A mechanical component, free to be moved, develops mechanical work by the action of a force

produced by electrical means [21]. The energy conservation law, together with governing laws of magnetism, electrical and mechanical equations, makes this possible to obtain the energy balance equation for the system, as follows:

$$W_e = W_{le} + W_{fe} + W_{em}, \tag{1}$$

where W_e is the input energy, W_{le} the energy losses, W_{fe} the stored magnetic field energy, and W_{em} the mechanical energy output. Note that the expressed mechanical and electrical quantities are positive for motor operation and negative for generator operation. Because frequency and speed are relatively low, a quasi-stationary electromagnetic field can be assumed and electromagnetic radiation losses can be neglected. Some fraction of the mechanical output is lost (W_{fw}), while the other part is stored in the mechanical system as kinetic energy (W_{sm}). Thus, the effective mechanical energy output is W_m, and is expressed as:

$$W_m = W_{em} - W_{fw} - W_{sm}. \tag{2}$$

The losses in the system can be caused by distinct causes, like losses in electrical conductors (I^2R losses), friction and ventilation (mechanical losses) and magnetic losses in the coupling field. A small and therefore ignored fraction of the loss is caused by the dielectric effect in the electrical insulating material. Thus, the following expression is obtained for the final energy balance equation:

$$W_e = \left(W_{le} + W_{fw}\right) + \left(W_{fe} + W_{sm}\right) + W_m. \tag{3}$$

Differential energy dW_e supplied by the source, neglecting magnetic losses, is given in (4), where voltage e is the reaction from the coupling field over the electrical system, u_s the coil supply voltage, R a resistance connected in series with the coil, and i the circuit current. Equation (4) shows also the relation between voltage e and magnetic linkage flux λ as follows:

$$dW_e = \left(u_s i - R i^2\right) dt = ie dt = i\, d\lambda. \tag{4}$$

Thus, as can be seen, if a change in flux linkage occurs, the system energy will also change. This variation can be promoted by means of a variation in excitation, a mechanical displacement, or both. The coupling field can be understood as a reservoir of energy, that receives it from the entrance system, the electrical system, and delivers it to the exit system, the mechanical system. Coupling field energy intakes brings on a reaction expressed by an induced voltage as:

$$e = \frac{d\lambda}{dt}. \tag{5}$$

Energy is a state function on a conservative system. If losses are ignored, balance energy can be written as in (6), where f_{em} is the mechanical force that produces the mechanical work dW_{em}, when a differential displacement dx occurs. Energy W_e, in a lossless device, with only one coil, depends on λ and x, as follows:

$$dW_e = dW_{fe} + f_{em}\, dx \;\Leftrightarrow\; dW_{fe} = i\, d\lambda - f_{em}\, dx. \tag{6}$$

A different energy entity, defined as co-energy W'_{fe}, with no physical meaning, can be expressed as follows:

$$W'_{fe}(i,x) = i\lambda - W_{fe}. \tag{7}$$

After mathematical manipulation of (7) and considering (6), one obtains (8), where it can be seen that the co-energy W'_{fe} depends on current i and position x:

$$\begin{aligned} dW'_{fe}(i,x) &= \lambda\, di + f_{em}\, dx \\ &= \frac{dW'_{fe}(i,x)}{\partial i}\, di + \frac{dW'_{fe}(i,x)}{\partial x}\, dx. \end{aligned} \tag{8}$$

Because i and x are independent variables, λ and f_{em} are given by the following equations, where L is the device magnetic inductance:

$$\begin{cases} \lambda = \dfrac{dW'_{fe}(i,x)}{\partial i} \Leftrightarrow L = \dfrac{\lambda}{i} \\ f_{em} = \dfrac{dW'_{fe}(i,x)}{\partial x} \end{cases}. \quad (9)$$

III. FINITE ELEMENTS MODELLING

For validation purposes, the proposed numerical methodology is used to analyze an electrovalve as a case study. The device is modelled through Flux2D©, from Cedrat [22]. It is assumed that the coil of the electrovalve has 1136 turns, with a resistance of 43 Ω. An exploded view of the device can be observed in Fig. 1. The axial view and respective physical dimensions are shown in Fig. 2.

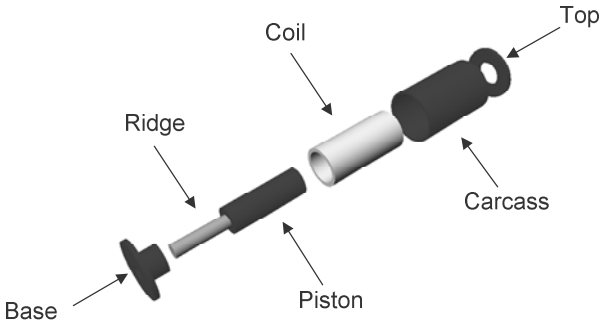

Fig. 1. Electrovalve exploded view.

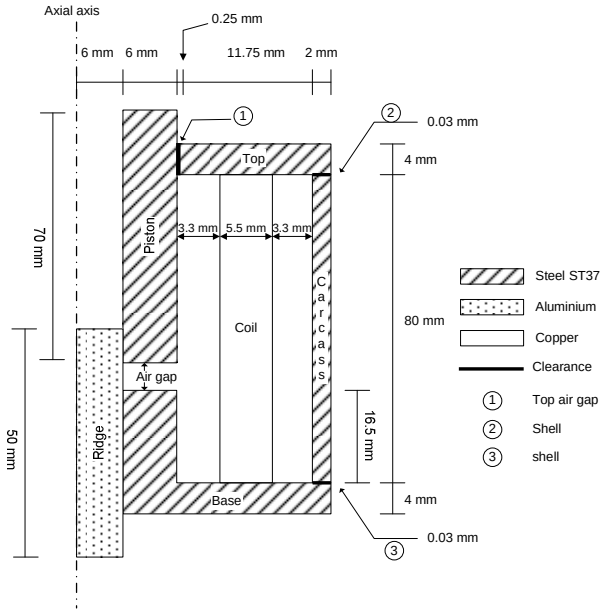

Fig. 2. Electrovalve axial view with physical dimensions.

A constructive detail of the finite element model is shown in Fig. 3. The different regions that compose this model are identified on it.

Concerning the introduction of materials connected with the different elements of the model, it is possible to recourse to a set of properties. For magnetic steels, the magnetization curve B - H is defined by means of the following relation:

$$B(H) = \mu_0 H + \frac{2J_s}{\pi} a\tan\left(\frac{\pi(\mu_r - 1)\mu_0 H}{2J_s}\right), \quad (10)$$

where μ_0 is the magnetic permeability of free space, μ_r the relative permeability and J_s the saturated magnetization. The expression is generally valid, but some errors can appear for curve values corresponding to the transition from the linear to the saturation region.

The finite element model has an infinite region with a half-circular form due to the device symmetry characteristic (see Fig. 4a), which is automatically generated as an extension of the classic analysis domain. The circular infinite region automatically receives cyclical conditions, making it physically dependent on the model limits; simultaneously, the inner part of the infinite region must present null Dirichlet conditions.

It is necessary to assign a specific property for each model region. All magnetic circuit parts are assumed as being steel made, while the screw thread and surrounding air regions are assumed as having the properties of vacuum (μ_r = 1), without any kind of associated current source. The coil region was also assigned the properties of vacuum, differing from the previous referred ones in the fact that a current source was considered. Each shell region (designated as 1 and 2 in Fig. 2) was assigned a constant and uniform thickness of 0.03 mm, with properties identical to the ones of the vacuum. Boundary conditions were also imposed for the analysis of the domain limit. Magneto-static problems formulation uses Dirichlet or Newmann boundary conditions, as in Fig. 4b. The circular infinite region automatically receives cyclical conditions, making it physically dependent on the model limits; simultaneously, the inner part of the infinite region must present null Dirichlet conditions.

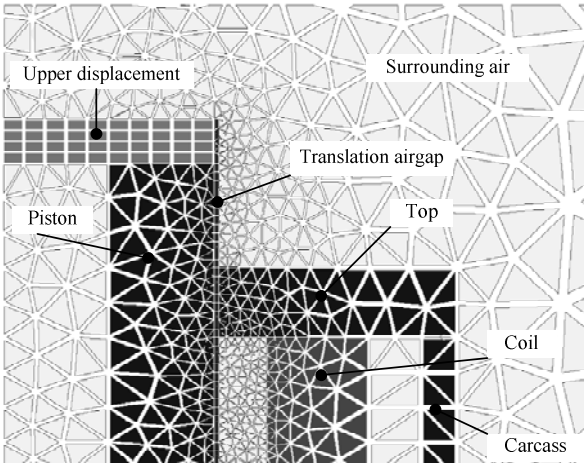

Fig. 3. Electrovalve FEM constructive detail.

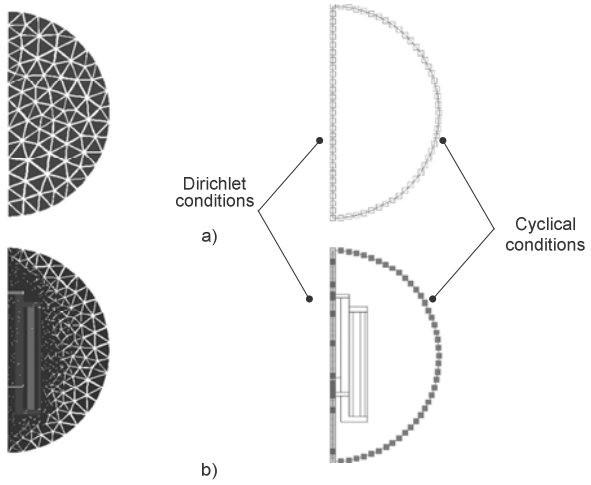

Fig. 4. Finite element mesh and boundary conditions: a) infinite region; b) electrovalve domain analysis.

The problem that authors intend to solve is a magneto-static problem, being all the computation carried out considering a steady-state situation. This fact means that neither the current nor the model geometry change during problem solving. Several static simulations have been performed. For each relative position x of the plunger, the finite elements model was analyzed, considering different excitation currents i. This task was performed using batch file programming under Flux2D©, which automatically reconfigures model parameters like plunger position x and current i, redefines model geometry and elements mesh, and collects the obtained data from the simulation process, saving it on computer hard disk for later processing proposes.

Data collected from simulations allowed the construction of a three-dimensional co-energy map, and from it, the attraction force, flux and inductance maps are properly derived, using (9). These characteristics are shown in Fig. 5, and can completely characterize the device behavior. Based on them, device numerical model can also be constructed and used to carry out the dynamical analysis. Each point of the co-energy map requires a static FEM simulation that takes approximately one minute. Notice that the case study is very simple, more complex geometries obviously will require more time. Another detail that must be observed is the co-energy map resolution. Some devices could require more points than others to define the map surface with a good resolution.

If devices geometrical parameters do not change, with the exception of the airgap length, there is no need to run the finite elements simulation again. Because the numerical model is implemented in a programming language (Matlab©) [23], simulation is more versatile and fast, in contrast with the finite elements tool.

IV. DMC NUMERICAL MODEL DEVELOPMENT

The proposed numerical model is based on the obtained values of the inductance and force maps. Using a representation of order $O(h^4)$ it is possible to obtain the centered difference expression (11) for the first derivative [24].

$$f'(x_i)=\frac{-f(x_{i+2})+8f(x_{i+1})-8f(x_{i-1})f(x_{i-2})}{12h}. \quad (11)$$

Derivative results can be improved either diminishing the step h or using a problem formulation of higher order with more points. Alternately, Richardson extrapolation uses two derivative values, obtained with different steps, to determine a third result. According to that, the extrapolation from expression (12) uses step $h_2 = h_1/2$.

$$f'(x_i)\approx\frac{4}{3}f'(x_i,h_2)-\frac{1}{3}f'(x_i,h_1). \quad (12)$$

The applied differentiation procedure returns as a result the force, flux, and inductance maps, which are shown in Fig. 5. The device non-

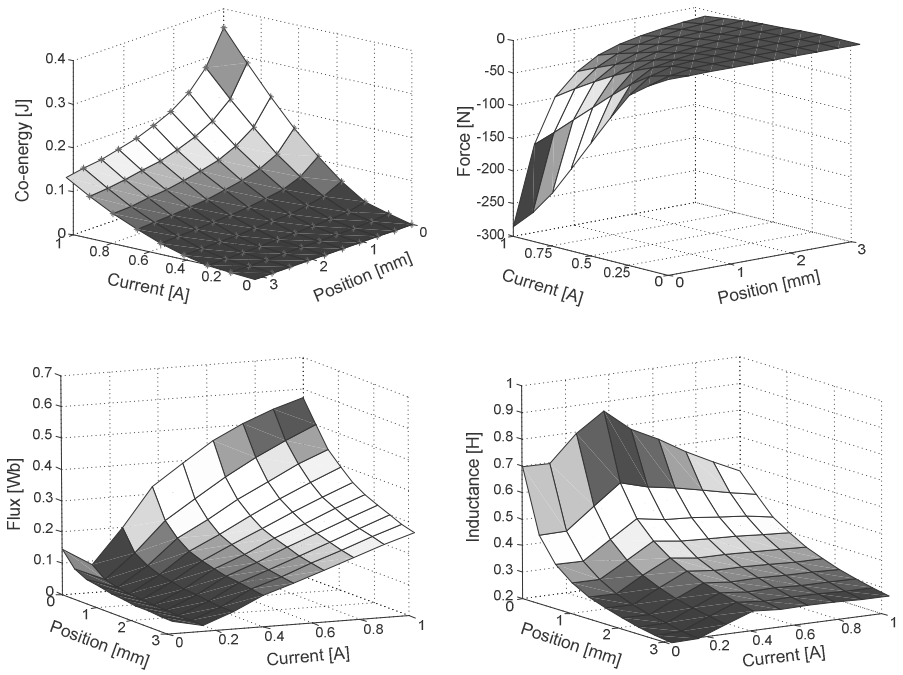

Fig. 5. Electrovalve three-dimensional maps: co-energy, force, flux and inductance.

linearity characteristic is shown in the previously referred maps. It is observable that inductance $L(i,x)$ and force $F(i,x)$ change not only with position x, but also with current i, exhibiting a strong influence of the magnetic circuit saturation. If these maps are used for device modeling, then simulation will take into account the actuator non-linearity.

The equation (13) describes the electromagnetic electrovalve behavior, being R the coil resistance and u_s the applied voltage:

$$u_s = R\, i(t) + \frac{dL(i,x)\, i(t)}{dt}. \qquad (13)$$

Because the inductance $L(i,x)$ is a function of the current i and position x, and in turn both function of time, the differentiation is carried through t, being terms di/dt and dx/dt placed in evidence, resulting:

$$u_s = \frac{di}{dt}\left[L(i,x) + i(t)\frac{\partial L(i,x)}{\partial i} \right] + . \\ + \frac{di}{dt}\left[i(t)\frac{\partial L(i,x)}{\partial x} \right] + Ri(t) \qquad (14)$$

Introducing parameters α and β as in:

$$\begin{cases} \alpha = L(i,x) + i\dfrac{\partial\ L(i,x)}{\partial i} \\ \beta = i\dfrac{\partial\ L(i,x)}{\partial x} \end{cases}, \qquad (15)$$

equation (14) becomes:

$$u_s = \alpha\frac{di}{dt} + \beta\frac{dx}{dt} + R\, i(t). \qquad (16)$$

Mathematical expressions (17) and (18) describe the dynamics of the electromechanical actuator, in which x, y, and a are, respectively, the plunger position, the velocity, and the acceleration, being M the plunger mass and F the produced attraction force.

$$a = \frac{1}{M} F \Leftrightarrow \frac{dy}{dt} = \frac{1}{M} F. \quad (17)$$

$$\frac{dx}{dt} = y. \quad (18)$$

The problem here under consideration is solved with Matlab© in two distinct steps. First, the plunger is allowed to move freely, and begins to do it from the considered initial position; this situation is described through the differential equations system (19). After, when stroke reaches its final position, it is considered that the movement is absent, and the velocity and acceleration will be zero. This situation is described by the differential equations system (20).

$$\begin{cases} \frac{dx}{dt} = y \\ \frac{dy}{dt} = \frac{1}{M} F \\ \frac{di}{dt} = -\frac{v_s - y\,\beta - R\,i}{\alpha} \end{cases}. \quad (19)$$

$$\begin{cases} \frac{dx}{dt} = 0 \\ \frac{dy}{dt} = 0 \\ \frac{di}{dt} = -\frac{v_s - y\,\beta - R\,i}{\alpha} \end{cases}. \quad (20)$$

The traditional solving methods for differential equations do not keep memory of the past solutions. Others, like the Adam family formulas for non-stiff problems and backward differences for stiff problems, take advantage from remembering past solutions. This formulations interpolate not only the solutions y_i, y_{i+1}, y_{i-p}, previously found, but also the new solution y_{i+1} using a polynomial $P(t)$. The solution at t_{i+1} is approached by the derivative of the following polynomial:

$$\left.\frac{dP}{dt}\right|_{t=t_{i+1}} = f\left(t_{i+1}, P\left(t_{i+1}\right)\right) = f\left(t_{i+1}, y_{i+1}\right) \quad . \quad (21)$$

The backward difference finite (BDF) family of formulas is obtained substituting the polynomial derivative at t_{i+1}, introducing coefficients α_p:

$$h\, f\left(t_{i+1}, y_{i+1}\right) = \bar{\alpha}_0\, y_{i+1} + \bar{\alpha}_1\, y_i + \ldots + \bar{\alpha}_p\, y_{i+1-p}. \quad (22)$$

The numerical differentiation formulas (NDF), defined by (23), and very close to the BDF, introduces some advantages. Here, k is a scalar parameter and the coefficients γ_k are given by $\gamma_k = \sum_{j=1}^{k} \frac{1}{j}$. Matlab© software implements NDF solving methodology in function ODE15S.

$$\sum_{m=1}^{n} \frac{1}{m} \nabla_{m+1}^{m} - h\, F\left(t_{n+1}, y_{n+1}\right) - k\, \gamma_k \left(y_{n+1} - y_{n+1}^{(0)}\right) = 0. \quad (23)$$

This function, or others like the ODE23, beyond solving with efficiency stiff problems, also has a good performance in solving non-stiff problems [23-25]. For each problem solving iteration, the values of α and β are obtained applying Spline interpolation and differential methods to the induction map. The dynamic simulation problem is solved using

```
[t,u,tev,uev,ie] = ode15s(@odemodelo_val1,
[0 tfim],uev,options,[],M,R,V1,interp_met);
```

where the parameter *odemodelo_val1* identifies the file that contains the numerical formulation made by a system of differential equations describing problem first phase. Before the system of differential equations can be evaluated, it is necessary to compute parameter $a(i,x)$ (α parameter), $b(i,x)$ (β parameter) and attraction force $f(i,x)$ for a specific system status (i,x). These operations are performed by the function *@odemodelo_val1* applying the previously described theoretical formulation. The determination of these parameters solves the system of differential equations for each problem phase. Equations (19) and (20) are described in Matlab as follows:

Problem phase I

```
dudt=zeros(size(u));
dudt(1)=u(2);
dudt(2)=f/M;
dudt(3)=(V1-u(2)*b-R*u(3))/a;
```

Problem Phase II

```
dudt=zeros(size(u));
dudt(1)= 0;
dudt(2)= 0;
dudt(3)=(V1-u(2)*b-R*u(3))/a;
```

The integration range is defined by vector [0 *tfim*], being the simulation end defined by *tfim*. Initial conditions are defined by the vector *uev* = [*x0 v0 i0*], where *x0* is the piston initial position, *v0* is the piston initial velocity, and *i0* the current in the solenoid coil at t = 0. The options of the ODE15s function are set with the *odeset* function:

```
options = odeset('OutputFcn',@odeplot,
'events',@events,'MaxStep',1e-4);
```

This function defines the output function *odeplot* that will represent the results graphically. The simulation process can be stopped by an event that is defined by the function *events*. This function is executed whenever it is necessary to check if the piston position reached the end of problem phase I, defined by *Vxcomuta*.

```
function [value,isterminal,direction] =
events(t,u,varargin)
    global VXcomuta;
    value = u(1)-VXcomuta;
    isterminal=1;
    direction=0
```

Finally, the parameter *MaxStep* defines the maximum integration step allowed. The *odemodelo_val1* also receives piston height (*M*), coil resistance (*R*), voltage source (*V1*), and the interpolation method to be used to collect data form maps.

At the end of problem phase I the following solution vectors are obtained: time (*t*), solution (*u*), event time (*tev*), last values of solution (*uev*), and wish event was occurred (*ie*). This information is saved and used as initial conditions of problem phase II. Now, the ODE15S function is used with the following configuration.

```
[t,u] = ode15s(@odemodelo_val2,
[tev tfim],uev,options,[],M,R,V1,interp_met);
```

This new problem stage is described by function *odemodelo_val2*.

After solving, the problem is possible to compute temporal evolution of the remaining variables associated with the electromechanical process of energy conversion. This task is performed applying interpolation methods in the respective variable map for each system state (*t*,*i*,*x*). This process allows us to compute the co-energy (*cw*), inductance (*l*), attraction force (*f*), and magnetic flux (*fl*).

Matlab application ends with the graphical exhibition of the dynamical results simulation. The solving process is shown in Fig. 6.

The process starts by loading the problem data and the initial approach to solve the problem, which corresponds to the plunger movement. When the plunger's stroke ends, another situation starts, and from this point forward to the end of the simulation, the plunger remains immobilized. Both problem stages are solved using ODE15S.

V. RESULTS ANALYSIS

The results obtained from the application of the proposed methodology to the case study can be visualized and compared with the ones obtained with the application of the finite elements tool, ignoring magnetic and iron losses. The results obtained considering the losses are also presented. The simulation was carried out considering a plunger mass *M* of 0.2 kg, an airgap length of 2.5 mm, and a DC voltage source of 30V, feeding a coil with 1136 turns and a resistance of 43 Ω. The plunger was initially considered immobilized, so that initial velocity and current were null. The established time for simulation was 70 msec, being 0.1 msec the maximum time step allowed in the FEM tool.

Results obtained from the proposed numerical model simulation are shown in Fig. 7, being also shown the ones obtained from Flux2D© simulation. The comparison between these results allows us to conclude that the first ones are closely fitting the second ones, corresponding to when the losses are neglected.

The DMC method allows that, after a non-

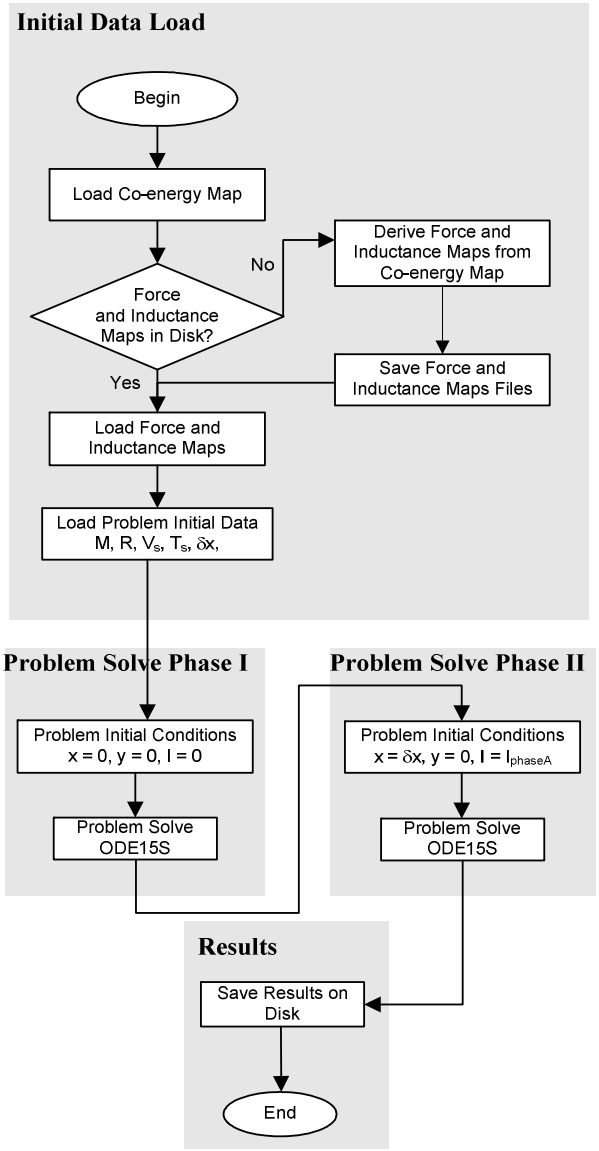

Fig. 6. Problem solving flowchart.

-geometric parameter change, like in voltage or coil resistance, the simulation can easily be repeated without solving the FEM model again. The proposed method is computationally efficient, taking less than two minutes, while the FEM tool takes about one hour to give equivalent results. Because the DMC problem is implemented using a high level programming language, changes can easily be introduced, allowing the validation of the device control strategy, for example.

The application of this methodology to a more complex device analysis, with more coils and/or a higher geometry complexity is not difficult, and the computation demands are completely independent from those complexities. From the analysis of Fig. 7, it can be noticed that the initial plunger movement is very small. As can be seen, current increases very quickly at this stage, but inductance stays almost constant. After reaching a first maximum, current decreases because inductance increases very quickly. When plunger movement stops, the current starts to increase again until it reaches a steady-state value, and because saturation effects are taken into account, inductance value decreases.

V. CONCLUSION

Dynamical simulation of electromagnetics actuators is usually accomplished with finite element tools. These kinds of tools appeal for high computational performance, are expensive, and take a long time to accomplish the simulation. Furthermore, FEM model complexity has high influence in the computation time and depends from the device's geometrical complexity. The previously described context turns the development and improvement of control methodologies hard to accomplish with FEM tools. Moreover, the development of advanced control methodologies could take advantage from an integration of electromagnetic device simulation with a numerical programming language.

This work proposes a simulation method to perform the dynamic behavior analysis of the electromagnetic actuators. This methodology uses a FEM software package at an early stage. After FEM model generation, several static simulations are performed to obtain the device co-energy map. The co-energy map must be obtained for each specific device. This approach is application specific to the electromagnetic actuator.

The co-energy map could be obtained through other methods like tube flux or experimentally. If device geometrical structure does not change, there is no need to run a new finite element model again. This data is used to make a device numerical model that, after being implemented in Matlab©, is used to observe the dynamical response of a case study device. From method implementation, we can conclude that computation effort to solve the problem is completely independent from the model geometry complexity. Introducing small changes, the proposed model could be easily applied to an actuator with a more

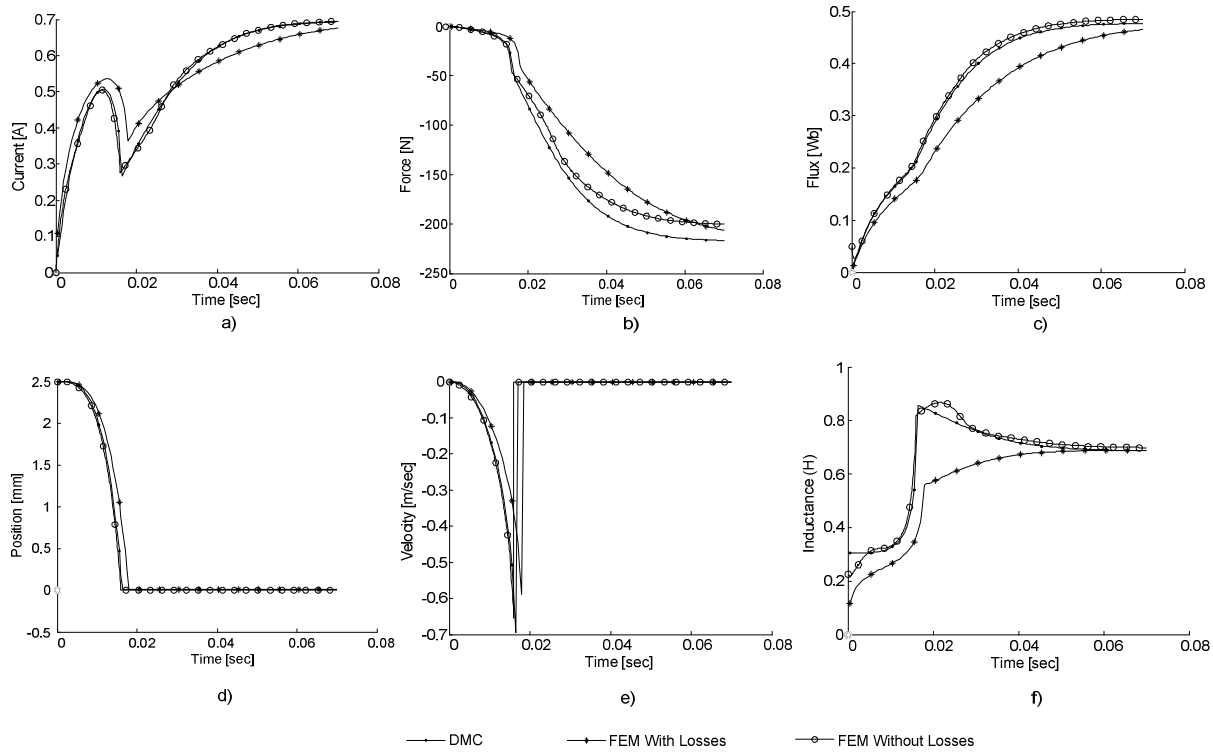

Fig. 7. Results as functions of time for a stroke of 2.5mm, with $u_s = 30\text{V}$, $R = 43\ \Omega$ and $M = 0.2$ Kg: a) current; b) force; c) flux; d) position; e) velocity; f) inductance.

complex geometry or with several excitation coils. The results can contribute to optimize actuator control methodology, with less computational effort. The mechanical load subsystem can be easily changed to simulate different mechanical loads or introduce friction effects.

REFERENCES

[1] H. C. Roters, *Electromagnetic Devices,* John Wiley and Sons, 1941.

[2] K. Srairi and M. Féliachi, "Electromagnetic Actuator Behavior Analysis Using Finite Element and Parameterization Methods," *IEEE Trans. Transactions on Magnetics*, vol. 31, no. 6, pp. 3497-3499, November 1995.

[3] G. Asche and Ph. K. Sattler, "Numerical Calculation of the Dynamic Behaviour of Electromagnetic Actuators," *IEEE Transactions on Magnetics*, vol. 26, no. 2, pp. 979-982, March 1990.

[4] K. Srairi and M. Féliachi, "Numerical Coupling Models for Analyzing Dynamic Behaviors of Electromagnetic Actuators," *IEEE Transactions on Magnetics*, vol. 34, no. 5, pp. 3608-3611, September 1998.

[5] Y. Xu and B. Jones, "A Simple Means of Predicting the Dynamic Response of Electromagnetic Actuators," *Mechatronics,* vol. 7, no. 7, pp. 589-598, October 1997.

[6] J. Faiz, J. Raddadi, and John W. Finch, "Spice-Based Dynamic Analysis of a Switched Reluctance Motor with Multiple Teeth per Stator Pole," *IEEE Transactions on Magnetics*, vol. 38, no. 4, pp. 1780-1788, July 2002.

[7] T. Tsukii, K. Nakamura, and O. Ichinokura, "SPICE Simulation of SRM Considering Nonlinear Magnetization Characteristics," *Electrical Engineering in Japan,* vol. 142, no. 1, pp. 50-56, 2003.

[8] U. Deshpande, "Two-Dimensional Finite-Element Analysis of a High-Force-Density Linear Switched Reluctance Machine Including Three-Dimensional Effects," *IEEE Transactions on Industry Applications*, vol. 36, no. 4, pp. 1047-1052, July/August 2000.

[9] X. D. Xue and K. W. E. Cheng, "A Self-Training Numerical Method to Calculate the Magnetic Characteristics for Switched Reluctance Motors Drives," *IEEE Transactions on Magnetics*, vol. 40, no. 2, pp. 734-737, March 2004.

[10] S. Kurz, J. Fetzer, T. Kube, G. Lehner, and W. M. Rucker, "BEM-FEM Coupling in Electromagnetics: A 2-D Watch Stepping Motor

Driven by A Thin Wire Coil," *ACES Journal*, vol. 12, no. 2, pp. 135-139, 1997.

[11] B. Parreira, S. Rafael, A. J. Pires, and P. J. Branco, "Obtaining the Magnetic Characteristics of an 8/6 Switched Reluctance Machine: From FEM Analysis to the Experimental Tests," *IEEE Transactions on Industrial Electronics*, vol. 52, no. 6, pp. 1635-1643, December 2005.

[12] K.Takayama, Y. Takasakiomoyuki, R. Ueda, and T. Sonoda, "Thrust Force Distribution on the Surface of Stator and Rotor Poles of Switched Reluctance Motor," *IEEE Transactions on Magnetics*, vol. 25, no. 5, pp. 3997-3999, September 1989.

[13] I. Boldea and S. A. Nasar, *Linear Electric Actuators and Generators*, Cambridge University Press, UK, 1997.

[14] S. Mcfee and D. A. Lowther, "Towards accurate and consistent force calculation in finite element based computational magnetostatics," *IEEE Transactions on Magnetics*, vol. 23, no. 5, pp. 3771-3773, September 1987.

[15] W. Muller, "Comparison of different methods of force calculation," *IEEE Transactions on Magnetics*, vol. 26, no. 2, pp. 1058-1061, March 1990.

[16] J. L. Coulomb, "A methodology for the determination of global electromechanical quantities for a finite element analysis and its application to the evaluation of magnetic forces, torques and stiffness," *IEEE Transactions on Magnetics*, vol. 19, no. 6, pp. 2514-2519, November 1983.

[17] P. P. Silvester and R. L. Ferrari, *Finite elements for electrical engineer*, Cambridge University Press, 1996.

[18] A. E. Santo, M. R. A. Calado, and C. M. P. Cabrita, "Variable Reluctance Linear Actuator Dynamics Analysis Based on Co-energy Maps for Control Optimization," *the Linear Drives for Industry Application*, Kobe-Awaji, Japan, September 2005.

[19] A. E. Santo, M. R. A. Calado, and C. M. P. Cabrita, "On the Influence of the Pole and Teeth Shapes on the Performance of Linear Switched Reluctance Actuator," *The International Journal for Computation and Mathematics in Electrical and Electronic Engineering* (accepted for publication), 2010.

[20] I. P. Hammond (1981): Energy Methods in Electromagnetism, *Oxford Science Publications*.

[21] A. E. Fitzgerald, *Electric machinery: The processes, devices, and systems of electromechanical energy conversion*, 3rd edition, McGraw-Hill, 1971.

[22] Flux2D (Version 7.40), *Translating motion tutorial*, Cedrat, 1999.

[23] C-M. Ong, Dynamic Simulation of Electric Machinery using Matlab/Simulink, *Englewood Cliffs, NI: Prentice-Hall*, 1998.

[24] S. C. Chapra, *Numerical methods for engineers*, McGraw-Hill International Editions, 1990.

[25] L. F. Shampine and M. W. Reichelt, "The MATLAB ODE Suite," *SIAM Journal on Scientific Computing*, vol. 18, pp. 1-22, 1997.

A. Espírito Santo received the Electrical Engineering degree from Universidade de Coimbra (FCTUC), Coimbra, Portugal, in 1996, the M.Sc. degree from the same institution, in 2002, and the Ph.D. degree from University of Beira Interior, Covilhã, Portugal, in 2008. He is currently Assistant Professor at UBI, Department of Electromechanical Engineering (DEM). His research area is instrumentation and control of actuators.

M. R. A. Calado received the Electrical Engineering degree from the Instituto Superior Técnico (IST), Lisbon, Portugal, in 1991, the M.Sc. equivalent degree and the Ph.D. degree from University of Beira Interior, Covilhã, Portugal, in 1996 and 2002, respectively.
She is currently Professor at UBI, Department of Electromechanical Engineering (DEM). She has about 50 scientific publications. Her research interests include electrical machines and actuators and numerical methods.

C. M. P. Cabrita received the Electrical and Computer Engineering and the Ph.D. degrees from the IST, Lisbon, in 1976 and 1988, respectively.
He was with Portuguese Railways from 1977 to 1978, in the electrical rolling stock division, and from 1978 to 1997, he was with IST, in the Electrical Machines Department. Since 1997, he has been with UBI, DEM, where currently he is a Full Professor. From 1978, he has also been a Consultant Engineer. He has about one hundred scientific publications. His research areas are electric traction and electrical machines and actuators.